Geometry of Einstein-Podolsky-Rosen Correlations

H. Chau Nguyen,[1,*] Huy-Viet Nguyen,[2,†] and Otfried Gühne[1,‡]
[1]*Naturwissenschaftlich-Technische Fakultät, Universität Siegen, Walter-Flex-Straße 3, 57068 Siegen, Germany*
[2]*Institute of Physics, Vietnam Academy of Science and Technology, 10 Dao Tan, Hanoi, Vietnam*

(Received 26 November 2018; revised manuscript received 17 April 2019; published 17 June 2019)

Correlations between distant particles are central to many puzzles and paradoxes of quantum mechanics and, at the same time, underpin various applications such as quantum cryptography and metrology. Originally in 1935, Einstein, Podolsky, and Rosen (EPR) used these correlations to argue against the completeness of quantum mechanics. To formalize their argument, Schrödinger subsequently introduced the notion of quantum steering. Still, the question of which quantum states can be used for EPR steering and which cannot remained open. Here we show that quantum steering can be viewed as an inclusion problem in convex geometry. For the case of two spin-1/2 particles, this approach completely characterizes the set of states leading to EPR steering. In addition, we discuss the generalization to higher-dimensional systems as well as generalized measurements. Our results find applications in various protocols in quantum information processing, and moreover they are linked to quantum mechanical phenomena such as uncertainty relations and the question of which observables in quantum mechanics are jointly measurable.

DOI: 10.1103/PhysRevLett.122.240401

In the simplest setting, the argument can be explained with two spin-1/2 particles, also called qubits, which are controlled by Alice and Bob at different locations [1,2]. The particles are in the singlet state,

$$|\psi\rangle_{AB} = \frac{1}{\sqrt{2}}(|01\rangle - |10\rangle), \tag{1}$$

where $|0\rangle = |\uparrow\rangle_z$ and $|1\rangle = |\downarrow\rangle_z$ denote the two possible spin orientations in the z direction. If Alice measures the spin of her particle in the z direction, then, depending on the obtained result, Bob's state will be in either state $|0\rangle$ or state $|1\rangle$, due to the perfect anticorrelations of the singlet state. On the other hand, if Alice rotates her measurement device to measure the spin in the x direction, Bob's conditional states are accordingly rotated to states $|\uparrow\rangle_x = (1/\sqrt{2})(|0\rangle + |1\rangle)$ or $|\downarrow\rangle_x = (1/\sqrt{2})(|0\rangle - |1\rangle)$ (see Fig. 1). So, by choosing her measurement, Alice can predict with certainty both the values of z and x measurements on Bob's side. According to Einstein, Podolsky, and Rosen (EPR), this means that both observables must correspond to "elements of reality." As the quantum mechanical formalism does not allow one to assign simultaneously definite values to these observables, EPR concluded that quantum mechanics is incomplete. As Schrödinger noted, Alice cannot transfer any information to Bob by choosing her measurement directions, but she can determine whether the wave function on his side is in an eigenstate of the Pauli matrix σ_x or σ_z. This *steering* of the wave function is, in Schrödinger's own words, "magic," as it forces Bob to believe that Alice can influence his particle from a distance [3,4].

The situation for general quantum states other than the singlet state can be formalized as follows [5]: Alice and Bob share a bipartite quantum state ϱ_{AB} and Alice performs different measurements. For each of Alice's measurement setting s and result r, Bob remains with a conditional state $\varrho_{r|s}$. These conditional states obey the condition $\sum_r \varrho_{r|s} = \varrho_B$, meaning that the reduced state $\varrho_B = \mathrm{Tr}_A(\varrho_{AB})$ on Bob's side is independent of Alice's choice of measurements. However, after characterizing the states

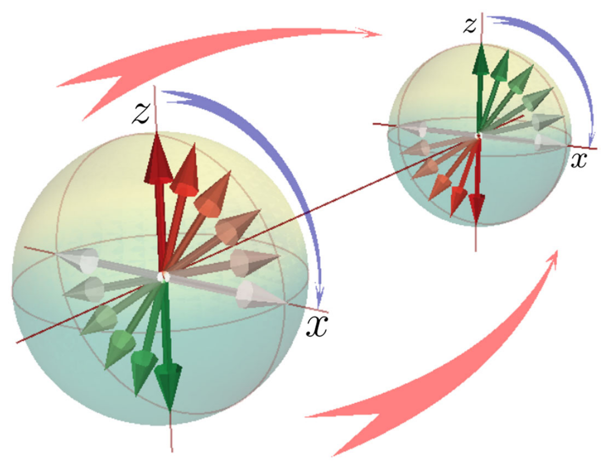

FIG. 1. Visualization of the steering phenomenon. Alice (in the forefront) measures the spin of her particle in an arbitrary direction. Because of the quantum correlations of the singlet state, Bob's state (in the back) is projected onto the opposite direction. Bob cannot explain this phenomenon by assuming preexisting states at his location, so he has to believe that Alice can influence his state from a distance.

$\varrho_{r|s}$, Bob may try to explain their appearance as follows: He assumes that initially his particle was in some states σ_λ with probability $p(\lambda)$, parametrized by some parameter λ. Then, Alice's measurement and result just gave him additional information on the probability of the states. This leads to states of the form [5]

$$\varrho_{r|s} = p(r|s) \int d\lambda p(\lambda|r, s)\sigma_\lambda. \tag{2}$$

This can be interpreted as if the probability distribution $p(\lambda)$ is just updated to $p(\lambda|r, s)$, depending on the classical information about the result and setting r, s. If a representation as in Eq. (2) exists, Bob does not need to assume any kind of action at a distance to explain the postmeasurement states $\varrho_{r|s}$. Consequently, he does not need to believe that Alice can steer his state by her measurements, and one also says that the state ϱ_{AB} is *unsteerable* or has a local hidden state (LHS) model. If such a model does not exist, Bob is required to believe that Alice can steer the state in his laboratory by some action at a distance. In this case, the state is said to be *steerable*.

So far, EPR steering has been observed in several experiments [6–13], but the question of which states can be used for EPR steering and which cannot remained, despite considerable theoretical effort [14–28], open. It is known that the set of steerable quantum states is strictly smaller than the set of entangled states and strictly larger than the set of states leading to a Bell inequality violation. But both entanglement and Bell nonlocality are not well understood [29,30]; only for the case of small dimensions or special families of states does the famous Peres-Horodecki criterion provide an exact characterization of the entangled states [31,32]. In this Letter we present a solution to the problem of steerability for the case of projective measurements carried out on two qubits. The generalization of the technique to higher-dimensional systems as well as taking into account generalized measurements is possible.

Conditional states and LHS models.—Let us characterize the conditional states and possible LHS models. For the former, we note that any bipartite quantum state ϱ_{AB} defines a map Λ from operators on Alice's space to operators on Bob's space via

$$\Lambda(X_A) = \mathrm{Tr}_A(\varrho_{AB} X_A \otimes \mathbb{1}_B). \tag{3}$$

This map characterizes the conditional states as follows: A result of a measurement setting is described by an effect $E_{r|s}$ which is an operator with positive eigenvalues not larger than one. The conditional state is then just given by $\varrho_{r|s} = \mathrm{Tr}_A(\varrho_{AB} E_{r|s} \otimes \mathbb{1}_B) = \Lambda(E_{r|s})$.

For our approach it is important that Λ has a clear geometrical meaning (see Fig. 2). The set of measurement

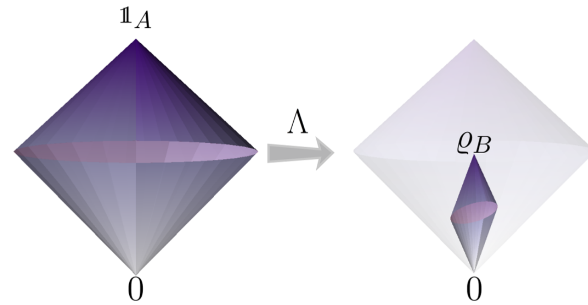

FIG. 2. Geometrical view of the map Λ. The set of measurement effects $\mathcal{M}_A$ on Alice's side is a four-dimensional double cone, where 0 and $\mathbb{1}_A$ correspond to the south and north pole and the equator is formed by the Bloch sphere. Under the action of the linear map Λ, this double cone is mapped onto a subset of itself, with $\Lambda(0) = 0$ and $\Lambda(\mathbb{1}_A) = \varrho_B$. The resulting set of steering outcomes is completely characterized by ϱ_B and the image of the equator under Λ.

effects on Alice's side, denoted by $\mathcal{M}_A = \{E_{r|s} | 0 \leq E_{r|s} \leq \mathbb{1}_A\}$, is a four-dimensional double cone, where 0 and $\mathbb{1}_A$ correspond to the south and north pole, and the pure effects of the form $E_{r|s} = |\psi\rangle\langle\psi|$ constitute the equator, which is nothing but Alice's Bloch sphere. The map Λ is linear and maps this double cone to a smaller double cone, denoted by $\Lambda(\mathcal{M}_A)$, which we call the set of steering outcomes [20]. For our purposes, we can assume without loss of generality that the map Λ is invertible; the proof of this and all forthcoming mathematical statements can be found in the Supplemental Material [33].

Let us now characterize the set of all possible LHS models. We first restrict our attention to projective measurements on two qubits; later we discuss the general case. Projective measurements are described by two orthogonal projectors $E_{+|s}$ and $E_{-|s}$ summing up to the identity $E_{+|s} + E_{-|s} = \mathbb{1}_A$. It is known that the LHS model Eq. (2) can be rewritten as [27]

$$\varrho_{\pm|s} = \Lambda(E_{\pm|s}) = \int_{\sigma\in\mathcal{B}_B} d\mu(\sigma) G_{\pm|s}(\sigma)\sigma, \tag{4}$$

with an integration over a probability distribution μ over all pure and mixed states in Bob's Bloch ball $\mathcal{B}_B$. The so-called response functions $G_{\pm|s}(\sigma)$ are positive and normalized as $G_{+|s} + G_{-|s} = 1$, which implies that they always have to obey the minimal requirement

$$\varrho_B = \Lambda(\mathbb{1}_A) = \int_{\sigma\in\mathcal{B}_B} d\mu(\sigma)\sigma. \tag{5}$$

In this scenario the set of all conditional states $\varrho_{\pm|s}$ that can be modeled with a LHS model is characterized by the probability distribution μ only. We call this set the capacity of μ and denote it by [20,27]

$$\mathcal{K}(\mu) = \left\{ K = \int_{\sigma\in\mathcal{B}_B} d\mu(\sigma) g(\sigma)\sigma : 0 \le g(\sigma) \le 1 \right\}. \quad (6)$$

Geometric approach.—In order to decide steerability, one has to compare the set of steering outcomes with the possible capacities. If one finds a LHS ensemble μ for which $\Lambda(\mathcal{M}_A)$ is a subset of $\mathcal{K}(\mu)$, then ϱ_{AB} is not steerable. On the other hand, if $\mathcal{K}(\mu)$ does not cover $\Lambda(\mathcal{M}_A)$ for all μ, then ϱ_{AB} is steerable.

Checking the inclusion relation between these sets is simplified by geometry; see Fig. 3. $\mathcal{K}(\mu)$ is a convex set which contains 0 and ϱ_B. The double cone $\Lambda(\mathcal{M}_A)$ is contained in this set if and only if its equator is contained in $\mathcal{K}(\mu)$. If we choose the metric appropriately, the equator of $\Lambda(\mathcal{M}_A)$ is a ball of radius one. Whether $\mathcal{K}(\mu)$ contains the ball or not can thus be determined by calculating the principal radius, defined as the minimal distance from the boundary of $\mathcal{K}(\mu)$ in the equator hyperplane to the center of the ball [22].

Our first main result is that the principal radius for a given probability distribution can be computed as a simple optimization problem, given by

$$r(\varrho_{AB},\mu) = \min_C \frac{1}{\sqrt{2}\|\mathrm{Tr}_B[\bar{\varrho}(\mathbb{1}_A \otimes C)]\|} \int_{\sigma\in\mathcal{B}_B} d\mu(\sigma)|\mathrm{Tr}_B(C\sigma)|, \quad (7)$$

where $\bar{\varrho} = \varrho_{AB} - (\mathbb{1}_A \otimes \varrho_B)/2$, the norm is given by $\|X\| = \sqrt{\mathrm{Tr}(X^\dagger X)}$, and the minimization runs over all single-qubit observables C on Bob's space. The proof of Eq. (7) relies on the Bloch representation and is given in the Supplemental Material [33].

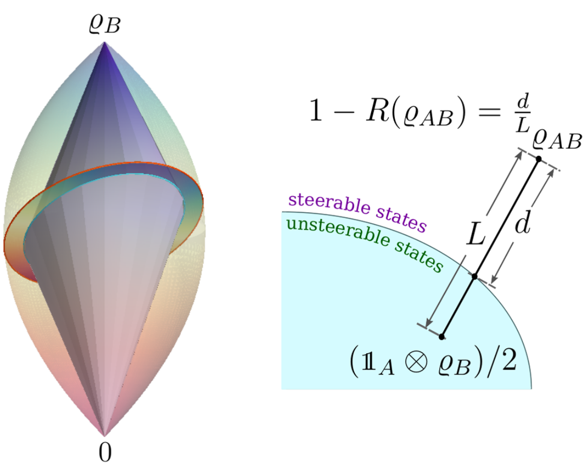

FIG. 3. Left: The geometrical interpretation of the critical radius. The capacity $\mathcal{K}(\mu)$ is a convex set containing 0 and ϱ_B. The double cone $\Lambda(\mathcal{M}_A)$ has 0 and ϱ_B as south and north pole, so $\Lambda(\mathcal{M}_A)$ is contained in $\mathcal{K}(\mu)$ if and only if its equator (cyan) is in $\mathcal{K}(\mu)$. This can be checked by computing the radius of $\mathcal{K}(\mu)$ in the appropriate plane and metric (red). Right: Operational meaning of the critical radius. $1 - R(\varrho_{AB})$ measures the distance from ϱ to the surface of unsteerable or steerable states relatively to $(\mathbb{1}_A \otimes \varrho_B)/2$.

Equation (7) allows us to compute the principal radius for a given distribution μ over states in Bob's Bloch ball. It remains to maximize this over all possible probability distributions. This leads to the critical radius,

$$R(\varrho_{AB}) = \max_\mu r(\varrho_{AB}, \mu). \quad (8)$$

In this way, we have reduced the characterization of steering to the computation of the critical radius and we can formulate: A two-qubit state can be used for EPR steering, if and only if the critical radius is smaller than one. All that remains to be done is to characterize the critical radius and to provide efficient methods for computing it. Showing the existence of the maximum in Eq. (8) requires careful continuity arguments as explained in the Supplemental Material [33].

Properties of the critical radius.—The first interesting property of the critical radius is its scaling. Given a two-qubit state, we can consider a family of states by mixing it with a special kind of separable noise,

$$\varrho_\alpha^{\mathrm{noise}} = \alpha\varrho_{AB} + (1-\alpha)\frac{\mathbb{1}_A}{2} \otimes \varrho_B, \quad (9)$$

where $0 \le \alpha \le 1$. For these states, we can show that

$$R(\varrho_\alpha^{\mathrm{noise}}) = \frac{1}{\alpha} R(\varrho_{AB}). \quad (10)$$

This implies that computing the critical radius for ϱ_{AB} also gives its values on the entire line in the state space parametrized by $\varrho_\alpha^{\mathrm{noise}}$. This scaling sheds light on the operational meaning of the critical radius: $1 - R(\varrho_{AB})$ measures the distance from ϱ_{AB} along this line to the border between steerable and unsteerable states relatively to $(\mathbb{1}_A \otimes \varrho_B)/2$.

The second important property is the symmetry of the critical radius. Given a state ϱ_{AB}, we consider the family of states

$$\tilde{\varrho} = \frac{1}{\mathcal{N}}(U_A \otimes V_B)\varrho_{AB}(U_A^\dagger \otimes V_B^\dagger), \quad (11)$$

where U_A is a unitary matrix on Alice's side, V_B is an invertible matrix on Bob's side, and $\mathcal{N}$ denotes the normalization. For this family of states one can show that $R(\varrho_{AB}) = R(\tilde{\varrho})$. This symmetry of the critical radius thus generalizes and formalizes quantitatively the early observation that the existence of a LHS model is invariant under Alice's local unitary and Bob's local filtering operations [18,19,45]. One may ask to what extent a mixed two-qubit state can be simplified with transformations as in Eq. (11). The answer is that any entangled state can be brought into a canonical form without changing its critical radius. In the canonical form, $\varrho_B = \mathbb{1}_B/2$ is maximally mixed and, in addition, all two-body correlations vanish, up to the diagonal ones, $s_i = \mathrm{Tr}(\varrho_{AB}\sigma_i \otimes \sigma_i)$ for $i = x,\ y,\ z$. So the critical radius of a state is uniquely determined by six parameters, coming from the reduced state of Alice, parametrized by $a_i = \mathrm{Tr}(\varrho_{AB}\sigma_i \otimes \mathbb{1}_B)$ and by a diagonal 3×3 matrix T.

Some facts about steering follow directly from the two properties mentioned above. First, as any pure entangled state $|\psi\rangle$ is equivalent to a Bell state in the sense of Eq. (11), one can easily show that $R(|\psi\rangle\langle\psi|) = 1/2$. Second, the previous properties allow for characterizing the convex sets $Q_t = \{\varrho_{AB} : R(\varrho_{AB}) \geq t\}$ and one can, for some cases, compute the tangent hyperplanes, resulting in optimal steering inequalities. Finally, generalizing Eq. (11), R is also invariant under the inversion of the Bloch sphere of either of the parties. This is rather surprising as entanglement of two-qubit states is equivalent to the occurrence of negative eigenvalues after partial transposition [31,32], which can be seen as a local inversion of the Bloch sphere. So, entanglement and quantum steering are, in fact, types of quantum correlations with fundamentally different mathematical structures.

Computation of the critical radius.—For practical convenience, the calculation of the critical radius of a generic state is carried out starting from its canonical form. Then, in order to evaluate Eq. (8) one needs to characterize the possible distributions μ. Instead of maximizing over all probability distributions on the Bloch ball, we approximate the ball by inner or outer polytopes as illustrated in Fig. 4. Crucially, for the special function in Eq. (7) one can show that optimizing over probability distributions supported at the vertices of the outer (inner) polytope leads to an upper (lower) bound R_{out} (R_{in}) for the critical radius. One may even simplify the calculation: If the inner polytope is chosen to have inversion symmetry, one has $R_{\mathrm{in}} \leq R(\varrho_{AB}) \leq R_{\mathrm{in}}/r_{\mathrm{in}}$, where r_{in} is the inscribed radius of the polytope. Then the relative difference between the bounds depends on the polytope only and not on details of the state. This bound also shows that as r_{in} converges to 1 one obtains an asymptotically exact value for $R(\varrho_{AB})$.

For a given polytope with N vertices, the calculation of the critical radius proceeds as follows: The capacity $\mathcal{K}(\mu)$ is a polytope in the four-dimensional space with $O(N^3)$ facets. When computing the critical radius, it suffices to consider the finite set of operators C that correspond to normal vectors of these facets, and these operators do not depend on the probability distribution on the polytope. As a consequence, the optimization over probability distributions is formulated as a linear program of finite size.

To illustrate the power of the method, we show examples of two-dimensional random cross sections of the set of two-qubit states; see Fig. 5. We observe that the computed upper and lower bounds for the critical radius are very tight even when a polytope with 252 vertices was used. A detailed discussion including further examples of states is given in the Supplemental Material [33].

Prior to our work, certain necessary and sufficient conditions for steerability were proposed [25,26], but their computability cannot be generally illustrated. There have been also attempts in estimating the boundary of the set of unsteerable states for special families of states with semidefinite programming (SDP) [16,23,28,46]. However, the SDP size increases exponentially with the number of

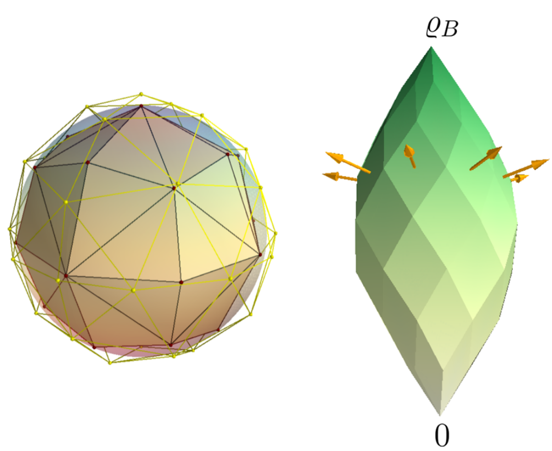

FIG. 4. Left: In order to characterize all probability distributions on the Bloch sphere, one can use inner and outer approximations of the sphere by polytopes. For the polytopes and the optimization problem in Eq. (7) it suffices to consider probability distributions supported at the extremal points. Right: For a given polytope, the capacity $\mathcal{K}(\mu)$ is a polytope again. Consequently, when computing the principal radius it suffices to consider the (finite) set of directions corresponding to the faces of the capacity polytope.

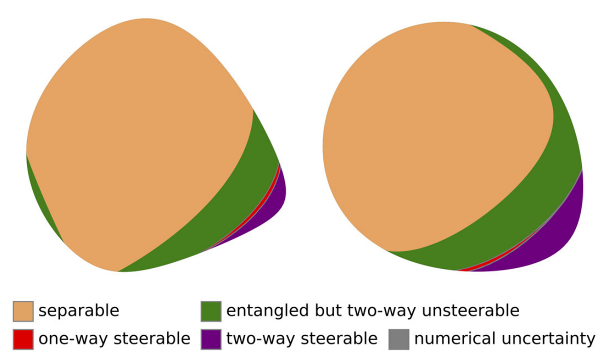

FIG. 5. Two two-dimensional random cross sections of the set of all two-qubit states. As EPR steering is not symmetric under the exchange of Alice and Bob, one can distinguish different classes of steerable states. The colors denote the set of separable states (characterized by the partial transposition [31,32]), entangled states that are unsteerable, one-way steerable states (Alice to Bob or vice versa), and two-way steerable states (Alice to Bob and vice versa). The very thin gray areas denote the states where the used numerical precision was not sufficient to make an unambiguous decision.

measurements used to approximate the set of all measurements. This limitation hinders the accurate locating of the boundary even for special choices of cross sections. Contrary to that, here we obtained a linear program, of which the size increases cubically with the number of approximated points. Both lower bound and upper bound with a predefined difference less than 1% for the critical radius of a generic state can be easily obtained in a reasonable computational time. Our implementation is available at a public repository [47].

Finally, we note that certain analytical bounds for the critical radius can also be derived from our approach. For example, for a state in the canonical form, it can be shown that

$$2\pi N_T|\det(T)| \geq R(\varrho_{AB}) \geq \frac{2\pi N_T|\det(T)|}{1+\|T^{-1}\vec{a}\|}, \qquad (12)$$

where $\vec{a}=(a_x,a_y,a_z)$ is the Bloch vector of Alice's reduced state, $N_T^{-1}=\int dS(\vec{n})[\vec{n}^T T^{-2}\vec{n}]^{-2}$ and the integration runs over the surface of the unit sphere. If $\vec{a}=0$, these bounds recover the exact formula for the critical radius of Bell diagonal states [21,22].

Generalized measurements and higher-dimensional systems.—A similar formula for the principal and critical radius can be derived for generalized measurements [i.e., positive operator-valued measures (POVMs)] and higher-dimensional systems, despite their more complicated geometry. As we explain in the Supplemental Material [33], many properties of the critical radius, such as its scaling and its symmetry, still hold. The fundamental question arises of whether generalized measurements are more useful for steering than the standard projective measurements considered so far. For two qubits, numerical estimation of the principal radii for POVMs provides clear evidence that, for a generic probability distribution μ, the principal radius for POVMs is the same as that for projective measurements. This encourages us to conjecture that POVMs do not give any advantage in EPR steering for the case of two-qubit states.

Discussion.—EPR steering is an asymmetric phenomenon where Bob, contrary to Alice, has well-characterized measurements. Consequently, the underlying correlations find applications in nonsymmetric scenarios of quantum information processing, such as one-sided device-independent quantum key distribution [48] or subchannel discrimination [49]. Clearly, our solution to the steering problem helps to understand and optimize these applications and their experimental realizations.

In addition, there are far-ranging consequences. First, it has been established that steering is in one-to-one correspondence with the question of which measurements in quantum mechanics can be jointly measured [45,50–52]. Second, recent works established close connections between quantum steering and entropic uncertainty relations [53,54]. Joint measurability and entropic uncertainty relations are central for many applications of quantum physics, such as the security of quantum key distribution [55]. We expect that our results and methods presented here may shed new light on these topics in the near future.

We are grateful to Fabian Bernards, Francesco Buscemi, Shuming Cheng, Ana C. S. Costa, Michael J. W. Hall, Teiko Heinosaari, C. Jebaratnam, Sania Jevtic, X. Thanh Le, Antony Milne, V. Anh Nguyen, Q. Dieu Nguyen, Jiangwei Shang, Roope Uola, Howard M. Wiseman, Xiao-Dong Yu, and particularly N. Duc Le for helpful comments and discussions. We thank the authors of Ref. [28] for kindly providing us with their SDP data. This work was supported by the DFG and the ERC (Consolidator Grant No. 683107/TempoQ). H. C. N. also acknowledges the support by the Vietnam National Foundation for Science and Technology Development (NAFOSTED) under Grant No. 103.02-2015.48. H.-V. N. acknowledges the financial support of the International Centre of Physics at the Institute of Physics, Vietnam Academy of Science and Technology.

*chau.nguyen@uni-siegen.de
†nhviet@iop.vast.ac.vn
‡otfried.guehne@uni-siegen.de

[1] A. Einstein, B. Podolsky, and N. Rosen, Phys. Rev. **47**, 777 (1935).
[2] D. Bohm, *Quantum Theory* (Prentice-Hall, New York, 1951).
[3] E. Schrödinger, Letter to A. Einstein on 13th July 1935, *Eine Entdeckung von Ganz Außerordentlicher Tragweite*, edited by K. v. Meyenn (Springer, New York, 2011), p. 551.
[4] E. Schrödinger, Proc. Cambridge Philos. Soc. **31**, 555 (1935).
[5] H. M. Wiseman, S. J. Jones, and A. C. Doherty, Phys. Rev. Lett. **98**, 140402 (2007).
[6] B. Wittmann, S. Ramelow, F. Steinlechner, N. K. Langford, N. Brunner, H. Wiseman, R. Ursin, and A. Zeilinger, New J. Phys. **14**, 053030 (2012).
[7] D. J. Saunders, S. J. Jones, H. M. Wiseman, and G. J. Pryde, Nat. Phys. **6**, 845 (2010).
[8] V. Händchen, T. Eberle, S. Steinlechner, A. Samblowski, T. Franz, R. F. Werner, and R. Schnabel, Nat. Photonics **6**, 596 (2012).
[9] D. H. Smith, G. Gillett, M. de Almeida, C. Branciard, A. Fedrizzi, T. J. Weinhold, A. Lita, B. Calkins, T. Gerrits, H. M. Wiseman, S. W. Nam, and A. G. White, Nat. Commun. **3**, 625 (2012).
[10] A. J. Bennet, D. A. Evans, D. J. Saunders, C. Branciard, E. G. Cavalcanti, H. M. Wiseman, and G. J. Pryde, Phys. Rev. X **2**, 031003 (2012).
[11] N. Tischler, F. Ghafari, T. J. Baker, S. Slussarenko, R. B. Patel, M. M. Weston, S. Wollmann, L. K. Shalm, V. B. Verma, S. W. Nam, H. C. Nguyen, H. M. Wiseman, and G. J. Pryde, Phys. Rev. Lett. **121**, 100401 (2018).

[12] K. Sun, X.-J. Ye, J.-S. Xu, X.-Y. Xu, J.-S. Tang, Y.-C. Wu, J.-L. Chen, C.-F. Li, and G.-C. Guo, Phys. Rev. Lett. **116**, 160404 (2016).

[13] Y. Xiao, X.-J. Ye, K. Sun, J.-S. Xu, C.-F. Li, and G.-C. Guo, Phys. Rev. Lett. **118**, 140404 (2017).

[14] S. J. Jones, H. M. Wiseman, and A. C. Doherty, Phys. Rev. A **76**, 052116 (2007).

[15] M. F. Pusey, Phys. Rev. A **88**, 032313 (2013).

[16] P. Skrzypczyk, M. Navascues, and D. Cavalcanti, Phys. Rev. Lett. **112**, 180404 (2014).

[17] J. Bowles, T. Vertesi, M. T. Quintino, and N. Brunner, Phys. Rev. Lett. **112**, 200402 (2014).

[18] R. Gallego and L. Aolita, Phys. Rev. X **5**, 041008 (2015).

[19] M. T. Quintino, T. Vértesi, D. Cavalcanti, R. Augusiak, M. Demianowicz, A. Acín, and N. Brunner, Phys. Rev. A **92**, 032107 (2015).

[20] H. C. Nguyen and T. Vu, Phys. Rev. A **94**, 012114 (2016).

[21] S. Jevtic, M. J. W. Hall, M. R. Anderson, M. Zwierz, and H. M. Wiseman, J. Opt. Soc. Am. B **32**, A40 (2015).

[22] H. C. Nguyen and T. Vu, Europhys. Lett. **115**, 10003 (2016).

[23] D. Cavalcanti and P. Skrzypczyk, Rep. Prog. Phys. **80**, 024001 (2017).

[24] A. Rutkowski, A. Buraczewski, P. Horodecki, and M. Stobinska, Phys. Rev. Lett. **118**, 020402 (2017).

[25] B.-C. Yu, Z.-A. Jia, Y.-C. Wu, and G.-C. Guo, Phys. Rev. A **97**, 012130 (2018).

[26] B.-C. Yu, Z.-A. Jia, Y.-C. Wu, and G.-C. Guo, Phys. Rev. A **98**, 052345 (2018).

[27] H. C. Nguyen, A. Milne, T. Vu, and S. Jevtic, J. Phys. A **51**, 355302 (2018).

[28] M. Fillettaz, F. Hirsch, S. Designolle, and N. Brunner, Phys. Rev. A **98**, 022115 (2018).

[29] R. Horodecki, P. Horodecki, M. Horodecki, and K. Horodecki, Rev. Mod. Phys. **81**, 865 (2009).

[30] N. Brunner, D. Cavalcanti, S. Pironio, V. Scarani, and S. Wehner, Rev. Mod. Phys. **86**, 419 (2014).

[31] A. Peres, Phys. Rev. Lett. **77**, 1413 (1996).

[32] M. Horodecki, P. Horodecki, and R. Horodecki, Phys. Lett. A **223**, 1 (1996).

[33] See Supplemental Material at http://link.aps.org/supplemental/10.1103/PhysRevLett.122.240401 for all the rigorous statements, technical proofs, and generalization, which includes Refs. [34–44].

[34] S. Jevtic (private communication).

[35] N. Gisin, Helv. Phys. Acta **62**, 363 (1989).

[36] L. P. Hughston, R. Jozsa, and W. K. Wootters, Phys. Lett. A **183**, 14 (1993).

[37] V. Bogachev, *Measure Theory I & II* (Springer-Verlag, Berlin, 2007).

[38] R. T. Rockafellar, *Convex Analysis* (Princeton University Press, Princeton, NJ, 1970).

[39] S. Jevtic, M. Pusey, D. Jennings, and T. Rudolph, Phys. Rev. Lett. **113**, 020402 (2014).

[40] J. Bowles, F. Hirsch, M. T. Quintino, and N. Brunner, Phys. Rev. A **93**, 022121 (2016).

[41] K. R. Parthasarathy, *Probablity Measures on Metric Spaces* (Academic Press Inc., New York, 1967).

[42] R. F. Werner, J. Phys. A **47**, 424008 (2014).

[43] J. Barrett, Phys. Rev. A **65**, 042302 (2002).

[44] R. H. Hardin, N. J. A. Sloane, and W. D. Smith, Tables of spherical codes with icosahedral symmetry, http://NeilSloane.com/icosahedral.codes/.

[45] R. Uola, T. Moroder, and O. Gühne, Phys. Rev. Lett. **113**, 160403 (2014).

[46] D. Cavalcanti, L. Guerini, R. Rabelo, and P. Skrzypczyk, Phys. Rev. Lett. **117**, 190401 (2016).

[47] Gitlab repository: https://gitlab.com/cn611340/epr-steering.

[48] C. Branciard, E. G. Cavalcanti, S. P. Walborn, V. Scarani, and H. M. Wiseman, Phys. Rev. A **85**, 010301(R) (2012).

[49] M. Piani and J. Watrous, Phys. Rev. Lett. **114**, 060404 (2015).

[50] M. T. Quintino, T. Vertesi, and N. Brunner, Phys. Rev. Lett. **113**, 160402 (2014).

[51] R. Uola, C. Budroni, O. Gühne, and J.-P. Pellonpää, Phys. Rev. Lett. **115**, 230402 (2015).

[52] T. Heinosaari, J. Kiukas, D. Reitzner, and J. Schultz, J. Phys. A **48**, 435301 (2015).

[53] A. C. S. Costa, R. Uola, and O. Gühne, Phys. Rev. A **98**, 050104(R) (2018).

[54] T. Krivachy, F. Fröwis, and N. Brunner, Phys. Rev. A **98**, 062111 (2018).

[55] P. J. Coles, M. Berta, M. Tomamichel, and S. Wehner, Rev. Mod. Phys. **89**, 015002 (2017).